

# On the transition from surface to interior solvation in iodide–water clusters

Denise M. Koch, Gilles H. Peslherbe \*

*Department of Chemistry and Biochemistry, Centre for Research in Molecular Modeling, Concordia University,  
1455 de Maisonneuve Blvd. W., Montréal, Qué., Canada H3G 1M8*

Received 2 January 2002; in final form 22 March 2002

## Abstract

A quantitative investigation of surface vs. interior solvation in iodide–water clusters was performed by evaluating the potentials of mean force and structural properties of  $\text{I}^-(\text{H}_2\text{O})_n$  clusters ( $n = 32, 64$ ) from Monte Carlo simulations with both non-polarizable and polarizable model potentials. Simulation results clearly indicate that the iodide ion tends to reside at the surface of a water cluster of size 32, whereas entropy and polarization effects make the interior solvation state more likely for a cluster size of 64. This is consistent with previous analyses of cluster experimental and model data, which suggest a transition from surface to bulk behavior around a cluster size of 60. © 2002 Elsevier Science B.V. All rights reserved.

## 1. Introduction

Ionic hydration has been the focus of numerous studies over the years, due to its fundamental importance in chemistry [1], biology [2] and environmental science [3]. Despite this long-lasting interest, the molecular-level details of ionic hydration have yet to be fully understood. Recent developments in experimental and theoretical techniques pertaining to cluster studies offer new possibilities for probing these processes [4]. In particular, cluster studies provide means for detailed investigations of the role of individual solvent molecules in the solvation of ionic species. An

important issue in ionic cluster studies is the hydration structure of halide ions. Numerous experimental [5–9] and theoretical [10–15] studies suggest that large halide ions preferentially sit at the surface of small-to-medium sized aqueous clusters, rather than being fully surrounded by water molecules, as they would be in the liquid phase.

Previous theoretical studies have made a connection between the solvation structure of ions and the competing ion–solvent and solvent–solvent interactions [16–19]. For large halides, since the ion–water binding energy is of a similar magnitude as the water–water binding energy, the water molecules tend to bind to each other rather than to the ion, and the ion–water interaction is not strong enough for the ion to disrupt the relatively stable water network. A key question that

\* Corresponding author. Fax: +1-514-848-2868.

E-mail address: [gkp@alcor.concordia.ca](mailto:gkp@alcor.concordia.ca) (G.H. Peslherbe).

arises from the existence of surface solvation states for large halide ions in aqueous clusters pertains to the cluster size at which the solvation behavior of these ions converge to bulk, i.e. at what cluster size does the ion adopt an interior, bulk-like, solvation structure? Markovich et al. [8] analyzed the  $\Gamma^-(\text{H}_2\text{O})_n$  cluster ( $n=1-60$ ) vertical detachment energies and solvent electrostatic stabilization energies resulting from photoelectron spectra, and could not conclude with certainty whether the clusters were in an interior or a surface solvation state. More recently, Coe [20] combined small cluster experimental solvation data [8,9,17], the results of simulations in model polar solvent clusters of intermediate size [21], and limiting continuum dielectric trends for large clusters to determine the evolution of the ion solvation free energy from the smallest cluster size to bulk. This analysis predicts that a gradual transition from surface to interior solvation occurs over the range  $n=1-60$ , and the transition to bulk behavior occurs around  $n \sim 60$ .

In the present work, we perform a quantitative investigation of the thermodynamics of surface vs. interior solvation in  $\Gamma^-(\text{H}_2\text{O})_n$  clusters in order to identify the possible transition from surface to bulk behavior. A convenient coordinate for discriminating between surface and interior solvation is the distance between the ion and the solvent center of mass, which would be close to zero for an ideally spherically solvated interior ion, and obviously deviates significantly from zero for a surface solvation state [22]. We calculate the free energy change along this coordinate, i.e. as the ion is forced to move towards or away from the solvent cluster center of mass, by means of constrained Monte Carlo simulations with model potentials. These potentials of mean force (PMF), as well as cluster structural properties, are investigated for  $\Gamma^-(\text{H}_2\text{O})_n$  clusters ( $n=32, 64$ ) with both non-polarizable and polarizable model potentials in order to assess the importance of polarizability on the thermodynamics of the halide–water clusters [22,23]. A brief account of the model potentials and simulation procedure is given in the next section. This is followed by a discussion of our simulation results, and by concluding remarks.

## 2. Simulation procedure

The simulation procedure has been thoroughly described elsewhere [22,23], and only a brief summary is provided here. Canonical ensembles of cluster configurations are generated at a temperature of 200 K by the Metropolis Monte Carlo method [24]. Each new trial configuration is generated randomly by translating one water molecule in every Cartesian direction, and rotating it around its Euler angles. The range of displacements for each degree of freedom was chosen to ensure an overall configuration acceptance ratio of ca. 40% [22]. The data are collected – after proper equilibration – in the form of successive Markov chains. This procedure allows us to (a) account for evaporation of water molecules by discarding from data collection the chains in which evaporation of one or more water molecules has occurred, and (b) to ensure that multiple local minima are sampled by gradually heating the clusters to 500 K and cooling them down in between each new chain. Overall, 2–4 million configurations are generated in a given simulation.

Two classical intermolecular model potentials are employed in order to describe the solvent–solvent and solute–solvent interactions. The first model, hereafter referred to as OPLS, consists of the TIP4P water model [25] supplemented by optimized parameters for liquid simulations (OPLS) [23,26]. The second model, hereafter referred to as OPCS [23], involves a polarizable five-site water model and optimized parameters for cluster simulations (OPCS). The latter model employs a water model with gas-phase experimental geometry, a three-dimensional point charge distribution, a polarizable site and distributed repulsion–dispersion sites, while the ion carries a point charge, a polarization site and a repulsion–dispersion site [22,23]. The water–water and ion–water interactions are parameterized from experimental data supplemented by ab initio calculations for small clusters [23].

The potential of mean force  $W(r_{\text{cm}})$ , where  $r_{\text{cm}}$  denotes the distance between the ion and the solvent center of mass, is generated by means of statistical perturbation theory evaluation of free energy differences [27]. The distance between the

ion and the solvent center of mass is constrained to a given value  $r_{\text{cm}}$  in the course of Monte Carlo simulations via a Lagrange multiplier approach [24]. For each configuration in the ensemble, the ion is displaced so as to increase and/or decrease the distance between the ion and the solvent center of mass by an increment  $dr_{\text{cm}}$  of 0.2 Å, and the Helmholtz free energy or potential of mean force change is evaluated as

$$\begin{aligned}\Delta W(r_{\text{cm}}) &= W(r_{\text{cm}} + dr_{\text{cm}}) - W(r_{\text{cm}}) \\ &= -kT \ln \left\langle e^{-[U(r_{\text{cm}} + dr_{\text{cm}}) - U(r_{\text{cm}})]/kT} \right\rangle_{r_{\text{cm}}},\end{aligned}$$

where  $\langle \dots \rangle$  denotes the canonical ensemble average. In practice, we make use of the results of forward perturbation for a simulation constrained at the value  $r_{\text{cm}}$ , and those of backward perturbation for a simulation constrained at the value  $r_{\text{cm}} + dr_{\text{cm}}$ , and evaluate the free energy change by the acceptance ratio method of Bennett [28]. This procedure also allows us to estimate error bars in the potential of mean force from the two distinct ensemble averages obtained from the simulations [23]. In the present simulations, the total error in the potentials of mean force is  $\pm 0.2$  kcal/mol over the range of  $r_{\text{cm}}$  values 0–7 Å.

### 3. Results and discussion

The potential of mean force (PMF) profiles are shown in Fig. 1 for  $\text{I}^-(\text{H}_2\text{O})_n$  clusters ( $n = 32, 64$ ) with both model potentials. The curves for  $\text{I}^-(\text{H}_2\text{O})_{32}$  are quite broad and shallow, as seen from Figs. 1a and b, with a minimum at a distance between the ion and the solvent center of mass  $r_{\text{cm}}$  of  $\sim 2$  Å. Two minima appear in the PMF profiles of  $\text{I}^-(\text{H}_2\text{O})_{64}$ , shown in Figs. 1c and d, suggesting that two distinct solvation states may exist for this cluster size. Accordingly, the  $r_{\text{cm}}$  probability distribution  $P(r_{\text{cm}})$ , calculated from the PMF data as  $P(r_{\text{cm}}) = 4\pi r_{\text{cm}}^2 e^{-W(r_{\text{cm}})/kT}$  and shown in Fig. 2, suggest that only one solvation state is present for  $\text{I}^-(\text{H}_2\text{O})_{32}$ , but two distinct states may exist for  $\text{I}^-(\text{H}_2\text{O})_{64}$ .

Let us first turn our attention to  $\text{I}^-(\text{H}_2\text{O})_{32}$  for which only one solvation state seems to be inferred from the  $P(r_{\text{cm}})$  distributions. The PMF curves

shown in Figs. 1a and b exhibit a large range of  $r_{\text{cm}}$  values, between ca. 0.5 and 3.5 Å, for which the PMF profile appears flat, and representative structures corresponding to these  $r_{\text{cm}}$  values, which are displayed in Figs. 3a and b, suggest that  $\text{I}^-(\text{H}_2\text{O})_{32}$  is in a surface solvation state over this full range of  $r_{\text{cm}}$  values. Besides  $r_{\text{cm}}$ , a rather convenient coordinate for rigorous investigations of the solvation structure around ions is the angle  $\theta$  between individual solvent molecules, the ion and the aqueous cluster center of mass, as depicted in Fig. 4 [22]. Large deviations from the isotropic angular probability distribution  $P(\theta) = \sin \theta$  are an indication of surface solvation [22]. The angular probability distributions  $P(\theta)$ , displayed in Fig. 4a, are very similar for both  $r_{\text{cm}} = 0.8$  and 3.6 Å. In both cases, a few water molecules are found on the side of the ion opposite to the solvent center of mass, suggesting that the cluster is in a surface solvation state over this wide range of  $r_{\text{cm}}$  values. It must be noted that these clusters are not always spherical, as shown in Fig. 3a, such that the ion can still reside at the surface of the cluster while having a small  $r_{\text{cm}}$  value.

As mentioned earlier, two minima appear in the PMF curves for  $\text{I}^-(\text{H}_2\text{O})_{64}$ , as shown in Figs. 1c and d. The resulting  $P(r_{\text{cm}})$  distribution for the OPLS model potential, which is shown in Fig. 2c, peaks at distances between the ion and the solvent center of mass of ca. 2.2 and 4.4 Å, clearly indicating the existence of two distinct solvation states. Representative structures shown in Figs. 3c and d for the clusters at these two  $r_{\text{cm}}$  values obviously correspond to interior and surface solvation structures, respectively. The angular probability distributions shown in Fig. 4b also demonstrate that the water molecules are more or less isotropically distributed around the iodide at  $r_{\text{cm}} = 2.2$  Å, whereas a few molecules are found on the side of the ion opposite to the solvent center of mass for  $r_{\text{cm}} = 4.4$  Å. The latter distributions actually resemble those for  $\text{I}^-(\text{H}_2\text{O})_{32}$  in Fig. 4a, which we have shown to possess a surface solvation structure. Therefore, for a cluster size of 64, two distinct solvation states are present, and the angular probability distributions confirm that these states correspond to interior and surface solvation of iodide.

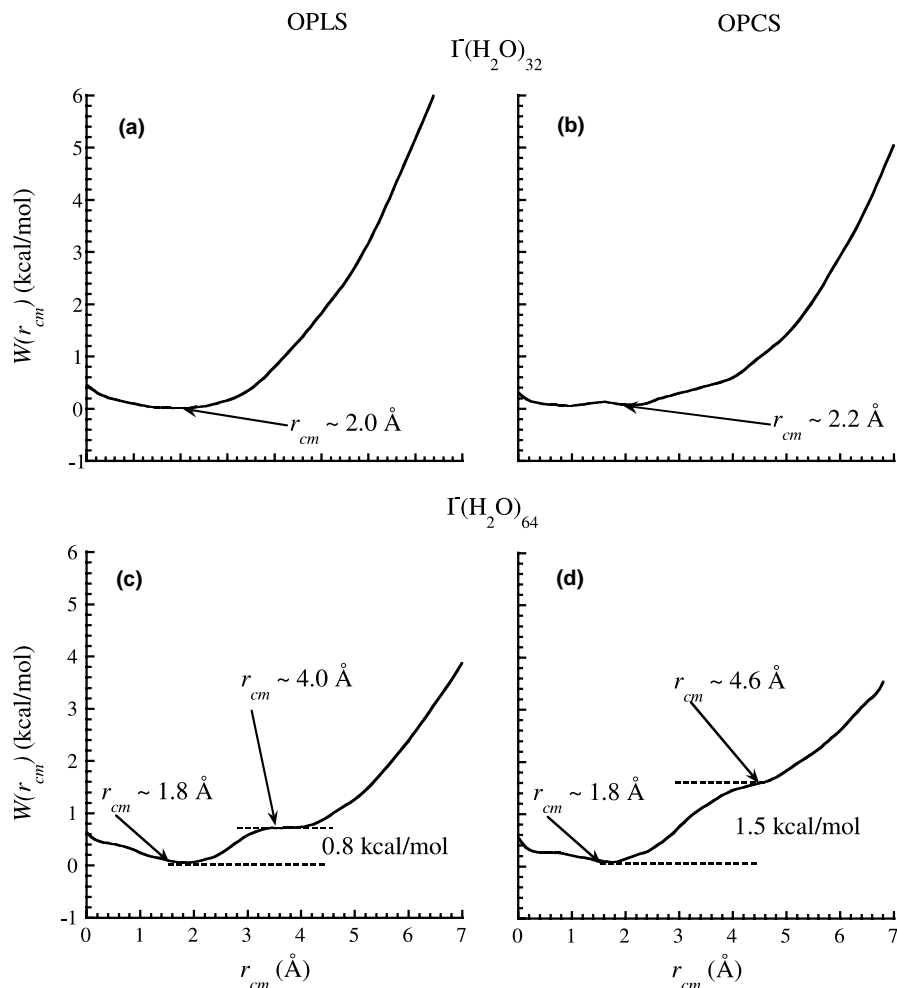


Fig. 1. Potentials of mean force  $W(r_{cm})$  generated with the OPLS (left panel) and OPCS (right panel) model potentials for: (a) and (b)  $\Gamma(\text{H}_2\text{O})_{32}$ , and (c) and (d)  $\Gamma(\text{H}_2\text{O})_{64}$ .

The equilibrium constant between the interior and surface states  $K_{I/S}$  can be evaluated as

$$K_{I/S} = \frac{[\text{Interior}]}{[\text{Surface}]} = \frac{\int_{\text{Int}} r_{cm}^2 e^{-W(r_{cm})/kT} dr_{cm}}{\int_{\text{Surf}} r_{cm}^2 e^{-W(r_{cm})/kT} dr_{cm}}$$

$$= \frac{\int_{\text{Int}} P(r_{cm}) dr_{cm}}{\int_{\text{Surf}} P(r_{cm}) dr_{cm}},$$

where the integrals run over the appropriate  $r_{cm}$  values for the interior and surface solvation states, and the boundary between the two states is chosen at the minimum between the two peaks in the  $P(r_{cm})$  distribution [23]. The resulting equilibrium

constant is  $1.6 \pm 0.4$  for the OPLS distribution of Fig. 2c, which indicates that the interior and surface states are almost equally likely for  $\Gamma(\text{H}_2\text{O})_{64}$ .

The effect of employing an explicitly polarizable model potential such as OPCS is to increase the free energy difference between the interior and surface solvation states of  $\Gamma(\text{H}_2\text{O})_{64}$  from 0.8 to 1.5 kcal/mol (cf. Figs. 1c and d), which largely increases the predominance of the interior state over the surface state, as seen from the  $P(r_{cm})$  distributions shown in Figs. 2c and d. With the OPCS model, the interior to surface equilibrium constant  $K_{I/S}$  is  $14.6 \pm 0.8$ , which represents a

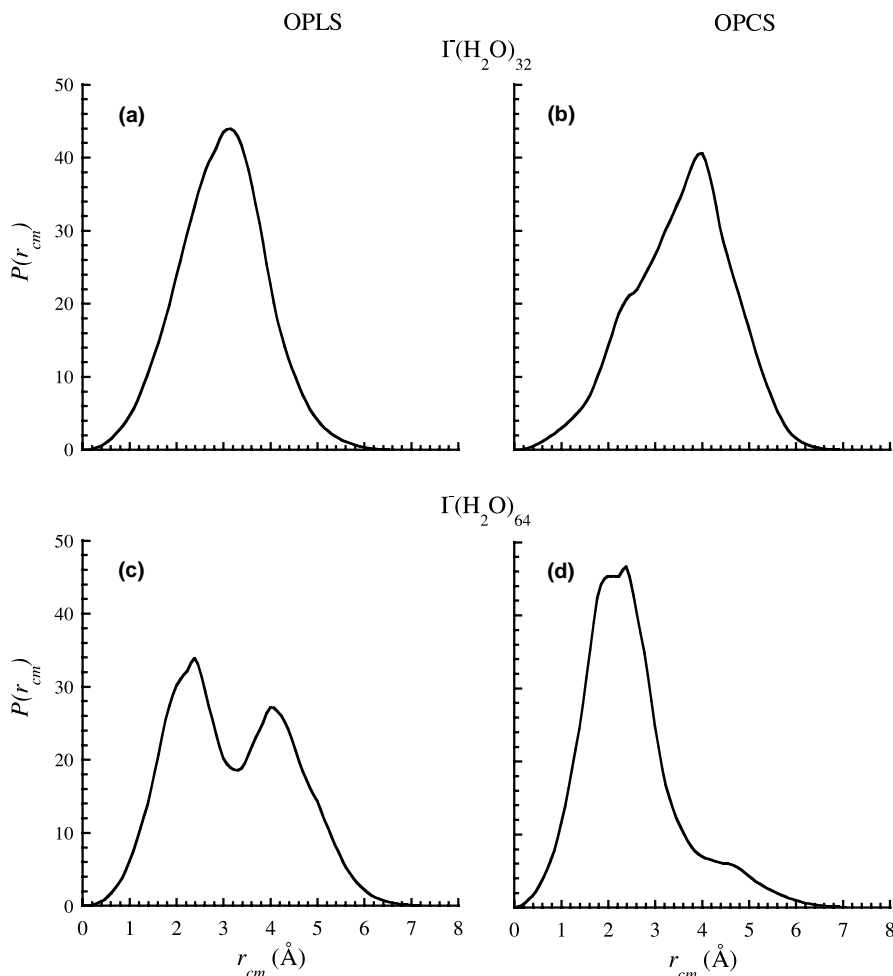


Fig. 2. Probability distributions of the distance between the ion and the solvent center of mass  $P(r_{cm})$  for: (a) and (b)  $\Gamma(\text{H}_2\text{O})_{32}$ , and (c) and (d)  $\Gamma(\text{H}_2\text{O})_{64}$  with both the OPLS (left panel) and OPCS (right panel) model potentials.

10-fold increase in the population of the interior state relative to that of the surface state when compared to the OPLS predictions. We should point out that, in a theoretical investigation of the ion coordination number for  $\text{Cl}^-(\text{H}_2\text{O})_n$  clusters, Stuart and Berne [29] found that polarizability favors surface solvation (up to a cluster size of 500), in contrast to our results for  $\Gamma(\text{H}_2\text{O})_n$ . We note that our own simulation results for  $\text{Cl}^-(\text{H}_2\text{O})_n$  yield results similar to those of Stuart and Berne, even though different forms of polarizable models are employed, and we are presently investigating the differences between chloride–water and iodide–water clusters [30].

To further our understanding of surface vs. interior solvation as a function of cluster size, we consider the  $P(r_{\text{HI}^-})$  probability distributions for  $\Gamma(\text{H}_2\text{O})_{32}$  and both solvation states of  $\Gamma(\text{H}_2\text{O})_{64}$  in Fig. 5.<sup>1</sup> The most prominent feature of the  $P(r_{\text{HI}^-})$  probability distributions is the striking resemblance between all curves. The only

<sup>1</sup> It is important to note that the cluster  $P(r_{\text{HI}^-})$  distributions vary from the liquid radial distribution functions by a factor of  $4\pi r^2$ , and the probabilities are normalized such that the integral distributions equal the number of solvent molecules in the cluster.

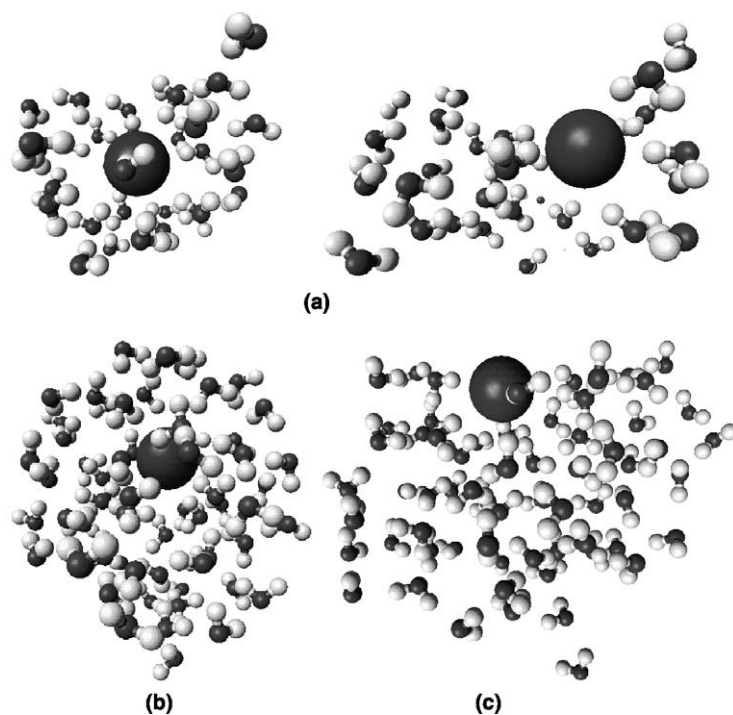


Fig. 3. Representative OPLS structures for: (a)  $\text{I}^-(\text{H}_2\text{O})_{32}$  at  $r_{\text{cm}} = 0.8$  and  $3.6 \text{ \AA}$ , (b) the interior solvation state of  $\text{I}^-(\text{H}_2\text{O})_{64}$  at  $r_{\text{cm}} = 2.2 \text{ \AA}$ , and (c) the surface solvation state of  $\text{I}^-(\text{H}_2\text{O})_{64}$  at  $r_{\text{cm}} = 4.4 \text{ \AA}$ .

difference between the  $\text{I}^-(\text{H}_2\text{O})_{64}$  interior and surface states is found in the  $P(r_{\text{HI}^-})$  probability of finding a water molecule further away than  $8 \text{ \AA}$  from the ion, which is close to the average globular radius of the interior state cluster of ca.  $7 \text{ \AA}$ . Obviously, more waters are found further away from the ion in the surface state. In turn, the probability of finding water molecules within  $4$  and  $8 \text{ \AA}$  is higher for the interior state than for the surface state because the iodide is fully surrounded by water molecules, as seen from Figs. 3b and c. The fact that the  $P(r_{\text{HI}^-})$  distributions are very similar for short distances is rather surprising, however. In principle, one would expect the solvation shell structure around iodide in the interior state to be better defined, and that the first solvation shell would contain more water molecules than in the surface solvation state (by first solvation shell, one actually refers to the first peak in the probability distribution functions and means the first few water molecules directly coordinated to the ions).

However, the  $\text{HI}^-$  probability distributions displayed in Fig. 5 indicate that iodide is directly coordinated with four water molecules in the first solvation shell in all cases considered, and do not show evidence of a secondary shell structure for the cluster sizes investigated. Previous studies have suggested that the first solvation shell around large halide ions is often dynamic [31]. In other words, the molecules in the first solvation shell may dynamically exchange with molecules in outlying shells. The  $P(r_{\text{HI}^-})$  distributions suggest that this type of dynamical exchange is present for  $\text{I}^-(\text{H}_2\text{O})_{32}$  and both solvation states of  $\text{I}^-(\text{H}_2\text{O})_{64}$ , since the first minima in the  $P(r_{\text{HI}^-})$  distributions do not go to exactly zero.

Since the  $r_{\text{HI}^-}$  probability distributions of  $\text{I}^-(\text{H}_2\text{O})_{64}$  are almost identical for the surface to interior states, let us now turn our attention to cluster enthalpies for both solvation states of the ion. Enthalpies can be obtained from our simulations as  $\Delta H = \langle \Delta V \rangle + nRT$ , where  $\langle \Delta V \rangle$  is the

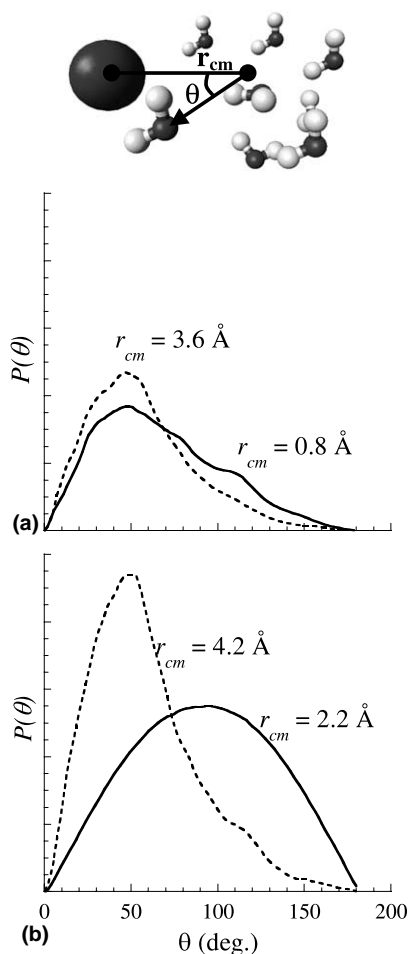


Fig. 4. Angular probability distributions  $P(\theta)$  for: (a)  $\text{I}^-(\text{H}_2\text{O})_{32}$  and (b)  $\text{I}^-(\text{H}_2\text{O})_{64}$  predicted by the OPLS model. As shown in the inset,  $\theta$  is defined as the angle between an individual solvent molecule, the ion and the solvent center of mass.

ensemble average of the cluster potential energy. The enthalpies for the surface to interic solvation states are  $-647$  and  $-646$  kcal/mol for the OPLS model, and  $-636$  and  $-634$  kcal/mol for the OPCS model, respectively. The enthalpy difference between the two solvation states for both model potentials is not significant within the error bar of 2 kcal/mol that we simply evaluated by varying the number of configurations employed to evaluate the ensemble averages. We note however that the surface state always seems to be energetically lower, even though we know from the interior to

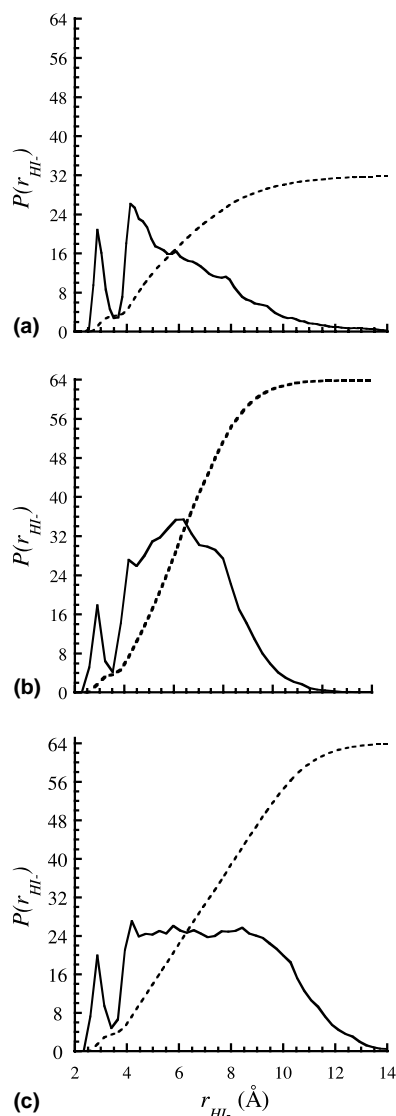


Fig. 5.  $\text{H-I}^-$  probability distributions functions for: (a)  $\text{I}^-(\text{H}_2\text{O})_{32}$ , (b) the interior state of  $\text{I}^-(\text{H}_2\text{O})_{64}$ , and (c) the surface state of  $\text{I}^-(\text{H}_2\text{O})_{64}$  as predicted by the OPLS model

surface equilibrium constants that it is not thermodynamically favored, a finding that is even more pronounced for OPCS. Therefore, the free energy difference between both states must be due to the difference in entropy between the interior and surface solvation structures. Furthermore, the larger free energy difference obtained with the OPCS model must be caused by a larger increase

in the system entropy due to polarization. As was suggested previously by Stuart and Berne [29], polarization allows for fluctuating dipoles such that the water molecules may remain more mobile, and thereby increase the entropy of the system.

#### 4. Concluding remarks

We performed a quantitative investigation of surface vs. interior solvation in iodide–water clusters in order to better identify the possible transition from surface solvation to bulk behavior. We evaluated the free energy change as a function of the distance between the ion and the solvent center of mass  $r_{\text{cm}}$  for  $\text{I}^-(\text{H}_2\text{O})_n$  clusters ( $n=32$  and 64) by means of constrained Monte Carlo simulations, using both OPLS and OPCS model potentials. The resulting potentials of mean force and  $r_{\text{cm}}$  probability distributions  $P(r_{\text{cm}})$  indicate that one solvation state is present for  $\text{I}^-(\text{H}_2\text{O})_{32}$  clusters, and two solvation states are present for  $\text{I}^-(\text{H}_2\text{O})_{64}$  clusters. For  $\text{I}^-(\text{H}_2\text{O})_{32}$ , the angular probability distributions  $P(\theta)$ , where  $\theta$  is the angle between individual solvent molecules, the ion and the aqueous cluster center of mass, clearly demonstrate that the ion resides at the surface of the cluster over the full range of  $r_{\text{cm}}$  values considered. The  $P(\theta)$  distributions also indicate that the two solvation states observed for the  $\text{I}^-(\text{H}_2\text{O})_{64}$  cluster correspond to distinct solvation states, an interior state and a surface state, with peaks in the probability distributions at  $r_{\text{cm}} \sim 2.2$  and 4.4 Å, respectively. This clearly indicates a transition from surface to interior solvation around a cluster size of 64, which is consistent with a detailed analysis of experimental and model data performed by Coe [20].

The effect of explicit polarization can be simply inferred by a direct comparison of the OPLS and OPCS simulation results. Including explicit polarization causes a significant increase in the free energy difference between the surface and interior solvation states of  $\text{I}^-(\text{H}_2\text{O})_{64}$ , which results in a large increase in the interior to surface equilibrium constants, from  $1.6 \pm 0.4$  for the OPLS model to  $14.6 \pm 0.8$  for the OPCS model. Although the enthalpy difference between the two solvation

states for both model potentials is not significant, the surface state tends to be slightly energetically favored, even though it is not thermodynamically favored, a finding that is even more pronounced for OPCS. This suggests that entropy and polarization effects, not too surprisingly, drive the ion towards the interior of the cluster around a cluster size of 64. A more comprehensive investigation of the thermodynamic and structural properties of halide–water clusters is underway.

#### Acknowledgements

This work was funded by research grants from the Natural Science and Engineering Research Council (NSERC) of Canada. Denise Koch is the recipient of NSERC and Concordia University Graduate Fellowships. Calculations were performed at the Centre for Research in Molecular Modeling (CERMM), which was established with the financial support of the Concordia University Faculty of Arts and Science, the Ministère de l'Éducation du Québec (MEQ) and the Canada Foundation for Innovation (CFI).

#### References

- [1] Y. Marcus, *Ion Solvation*, Wiley, New York, 1985.
- [2] G.W. Robinson, S.-B. Zhu, S. Singh, M.W. Evans, *Water in Biology, Chemistry and Physics: Experimental Overview and Computational Methodologies*, World Scientific, Singapore, 1996.
- [3] B.J. Mason, *The Physics of Clouds*, second ed., Oxford University Press, London, 1971.
- [4] E.R. Bernstein, *Chemical Reactions in Clusters*, Oxford University Press, New York, 1996.
- [5] P. Jayaweera, A.T. Blades, M.G. Ikononou, P. Kebarle, *J. Am. Chem. Soc.* 112 (1990) 2452.
- [6] P. Ayotte, G.H. Weddle, J. Kim, J. Kelley, M.A. Johnson, *J. Phys. Chem. A* 103 (1999) 443.
- [7] J.H. Choi, K.T. Kuwata, Y.B. Cao, M. Okumura, *J. Phys. Chem. A* 102 (1998) 503.
- [8] G. Markovich, S. Pollack, R. Giniger, O. Cheshnovsky, *J. Chem. Phys.* 101 (1994) 9344.
- [9] K. Hiraoka, S. Mizuse, S. Yamabe, *J. Phys. Chem.* 92 (1988) 3943.
- [10] W.L. Jorgensen, D.L. Severance, *J. Chem. Phys.* 99 (1993) 4233.
- [11] S.S. Xantheas, *J. Phys. Chem.* 100 (1996) 9703.

- [12] L.S. Sremaniak, L. Perera, M.L. Berkowitz, *Chem. Phys. Lett.* 218 (1994) 377.
- [13] H.D. Gai, G.K. Schenter, L.X. Dang, B.C. Garrett, *J. Chem. Phys.* 105 (1996) 8835.
- [14] T.N. Truong, E.V. Stefanovich, *Chem. Phys.* 218 (1997) 31.
- [15] J.E. Combariza, N.R. Kestner, J. Jortner, *J. Chem. Phys.* 100 (1994) 2851.
- [16] M. Arshadi, R. Yamaguchi, P. Kebarle, *J. Phys. Chem.* 74 (1979) 2599.
- [17] R.G. Keesee, A.W. Castleman Jr., *Chem. Phys. Lett.* 74 (1980) 139.
- [18] K. Liu, J.D. Cruzan, R.J. Saykally, *Science* 271 (1996) 929.
- [19] J.D. Cruzan, L.B. Braly, K. Liu, G. Brown, J.G. Loeser, R.J. Saykally, *Science* 271 (1996) 59.
- [20] J.V. Coe, *J. Phys. Chem. A* 101 (1997) 2055.
- [21] D.S. Lu, S.J. Singer, *Chem. Phys.* 105 (1996) 3700.
- [22] G.H. Peslherbe, B.M. Ladanyi, J.T. Hynes, *Chem. Phys.* 258 (2000) 201.
- [23] G.H. Peslherbe, B.M. Ladanyi, J.T. Hynes, *J. Phys. Chem. A* 104 (2000) 4533.
- [24] M.P. Allen, D.J. Tildesley, *Computer Simulation of Liquids*, Oxford University Press, New York, 1989.
- [25] W.L. Jorgensen, J. Chandrasekhar, J.D. Madura, R.W. Impey, M.L. Klein, *J. Chem. Phys.* 79 (1983) 926.
- [26] J. Chandrasekhar, D.C. Spellmeyer, W.L. Jorgensen, *J. Am. Chem. Soc.* 106 (1984) 903.
- [27] J.K. Buckner, W.L. Jorgensen, *J. Am. Chem. Soc.* 111 (1989) 2507.
- [28] C.H. Bennett, *J. Comput. Phys.* 22 (1976) 245.
- [29] S.J. Stuart, B.J. Berne, *J. Phys. Chem.* 100 (1996) 11934.
- [30] D.M. Koch and G.H. Peslherbe, manuscript in preparation.
- [31] S.H. Lin, P.C. Jordan, *J. Chem. Phys.* 89 (1988) 7492.